Photonic Technologies for Millimeter- and Submillimeter-Wave Signals

B. Vidal, T. Nagatsuma, N. J. Gomes, and T. E. Darcie

September 2012

Hindawi Publishing Corporation
Advances in Optical Technologies
Volume 2012, Article ID 925065, 18 pages
doi:10.1155/2012/925065

Review Article

Photonic Technologies for Millimeter- and Submillimeter-Wave Signals

B. Vidal,[1] T. Nagatsuma,[2] N. J. Gomes,[3] and T. E. Darcie[4]

[1] *Nanophotonics Technology Center, Polytechnic University of Valencia, 46022 Valencia, Spain*
[2] *Department of Systems Innovation, Graduate School of Engineering Science, Osaka University, Osaka 565-0871, Japan*
[3] *Broadband and Wireless Communications Group, University of Kent, Canterbury CT2 7NT, UK*
[4] *Department of Electrical and Computer Engineering, University of Victoria, Victoria, BC, Canada V8W 3P6*

Correspondence should be addressed to B. Vidal, bvidal@dcom.upv.es

Received 24 July 2012; Accepted 9 September 2012

Academic Editor: Kiyoshi Shimamura

Fiber optic components offer a competitive implementation for applications exploiting the millimeter-wave and THz regimes due to their capability for implementing broadband, compact, and cost-effective systems. In this paper, an outline of the latest technology developments and applications of fiber-optic-based technologies for the generation, transmission, and processing of high-frequency radio signals is provided.

1. Introduction

Optical fiber is an outstanding transmission medium which revolutionized data communications due to its unique combination of low loss and wide bandwidth [1]. Although originally targeted at long-distance communications, fiber optic technology has been applied to a wide range of fields, among them access networks, data centers, sensing, fiber lasers, illumination, imaging, and so forth. Another important, yet initially unforeseen, application for fiber optic technology was the interaction between optics and microwaves for applications such as radar, communications, warfare systems, and instrumentation. This area has become known as microwave photonics [2–6] and includes the photonic generation and distribution, processing, and monitoring of microwave signals, as well as photonic-assisted analog-to-digital conversion, to cite its main topics.

Features such as the low loss and wide bandwidth of fiber optic technology can be exploited to provide functions and capabilities to microwave systems that are very complex or even not implementable when carried out directly in the microwave domain. These advantageous characteristics are especially relevant when high frequency signals are considered given current limitations in the generation, processing, and distribution of millimeter- and submillimeter-wave signals.

The millimeter-wave region of the electromagnetic spectrum (Figure 1), also called the extremely high frequency range, (EHF), corresponds to radiofrequencies from 30 GHz to 300 GHz (i.e., wavelengths from 10 mm to 1 mm). The high frequency of the signals in this band as well as their propagation characteristics makes them useful for a variety of applications. However, the difficulty in generating and detecting signals as well as atmospheric attenuation in this band limits current applications. Existing applications include data transmission (high-bit rate wireless access networks), and radar (mainly benefiting from the beam width achievable with small antennas in applications such as short range automotive radars at 77 GHz as well as in scientific, military, security controls, and range and speed measurement for industrial applications).

Beyond the millimeter-wave band, and below infrared frequencies, there is a gap in the spectrum where the historic difficulties in generating and detecting signals have prevented the development of applications. This still little used frequency band is known as the submillimeter-wave band, far-infrared, or terahertz band, corresponding to radiofrequencies from 300 GHz to 3 THz (i.e., wavelengths

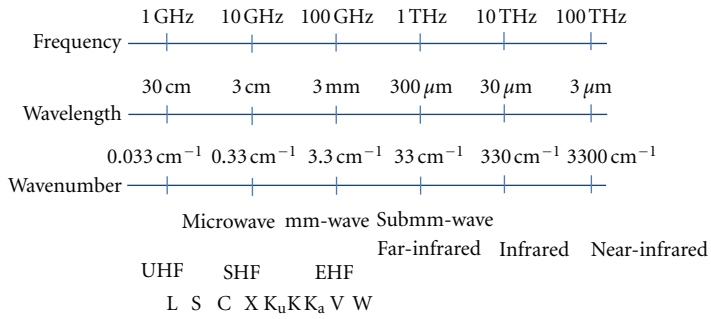

Figure 1: Electromagnetic spectrum and common band names.

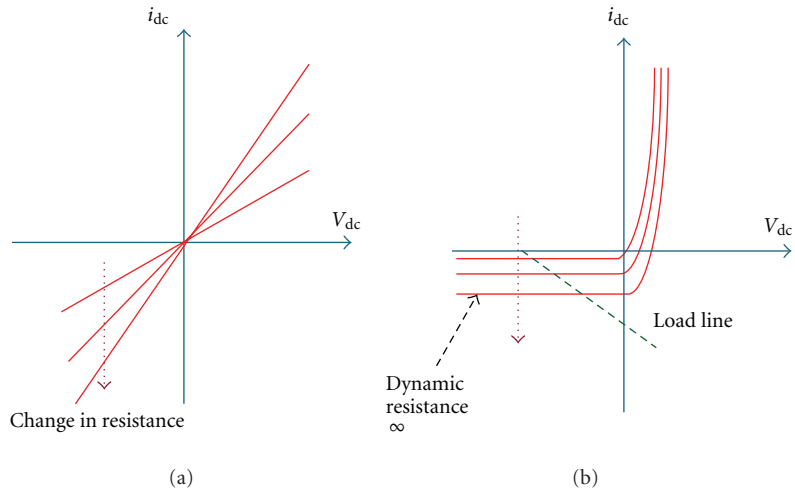

Figure 2: Typical dc I-V characteristics of (a) photoconductors and (b) photodiodes.

from 1 mm to 100 μm). Terahertz radiation has been long studied in fields such as astronomy and analytical science. However, recent technological innovations in photonics, electronics, and nanotechnology are resulting in a wide range of breakthroughs which have pushed THz research into the center stage [7–12].

In this paper, we explore and discuss several technologies, systems, and applications where fiber optic technology is showing competitive features in comparison to its electronic counterparts and is helping to widen the range of applications exploiting these frequency bands. The paper is organized as follows. Section 2 describes high bandwidth detectors and waveguides for the photonic generation of high-frequency signals. These are key components in implementing efficient fiber optic systems at millimeter- and submillimeter-wave frequencies. Section 3 is devoted to the application of fiber optic technology for data transmission and Section 4 to the exploitation of the submillimeter band by means of time and frequency spectroscopy. Finally, a conclusion is provided in Section 5.

2. Components

2.1. Photoconductors and Photodiodes for THz Generation and Detection. Photonic techniques have been essential in developing THz technologies with respect to signal generation and detection. The most fundamental and widely used devices are based on the optical-to-THz or THz-to-optical conversion using interaction media such as nonlinear optical (NLO) materials, photoconductors, and photodiodes. Typical NLO materials are crystals with large nonlinear susceptibility such as CdTe, ZnTe, GaP, LiNbO3, and DAST (4-dimethylamino-N-methyl-4-stilbazolium tosylate). Such materials offer the widest bandwidth in the signal generation and detection and the highest peak-power generation [13, 14]. There are no metallic electrodes nor antennas for NLO materials. However, because of their low conversion efficiency, NLO materials require intense illumination of light, which makes it difficult to introduce optical-fiber cables; THz systems with NLO materials are mostly based on free-space optics. Thus, in this section, we address photoconductor and photodiodes suitable for fiber-optic system applications.

Figure 2 shows typical dc current-voltage characteristics of a photoconductor and a photodiode, showing the change in the current-voltage curve under the illumination of infrared (IR) and visible light. The photoconductor is a conducting element whose conductance is controlled by the incident light. The response speed or the frequency bandwidth of the photoconductor is determined by the

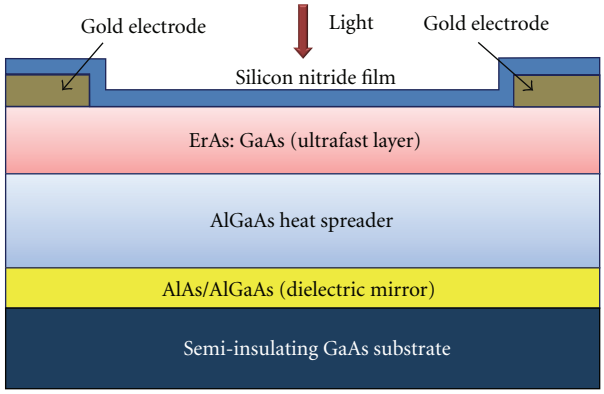

Figure 3: Example of layer structures for high-power GaAs-based photoconductors.

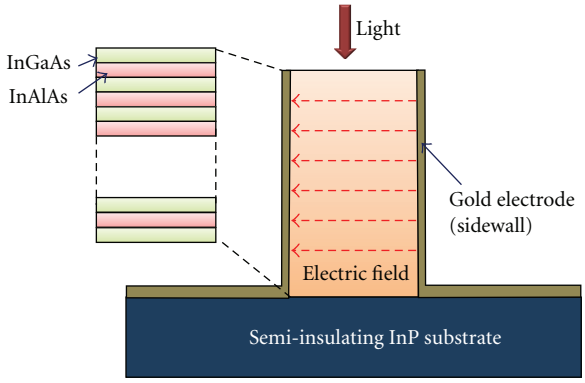

Figure 4: Example of device structures for high-power InGaAs-based photoconductors.

photogenerated carrier transit time and/or the carrier recombination time. To decrease the former time constant, there are two approaches; one is to reduce the gap distance between electrodes by deep-submicron lithography and the other is to apply a stronger electric field or voltage across the gap. In addition, an interdigitated finger structure can be introduced for the electrodes to ensure the sensitivity. In order to efficiently emit/receive THz waves into/from free space, the electrodes are directly integrated with planar antennas such as dipole, log-periodic, bow-tie, or spiral antennas.

The choice of photoconductive materials has been long studied since their first application for picosecond switching in the 1970's. Primary materials are low-temperature grown (LTG) GaAs and ErAs : GaAs (i.e., nanoparticles embedded in a GaAs matrix) for visible wavelength (700~800 nm) lasers (Figure 3). Heat spreading layers made of AlGaAs together with dielectric mirror layers have successfully been introduced to further enhance the THz emission and conversion efficiency [15]. For telecom wavelength (1550 nm) lasers, LTG InGaAs, ErAs : InGaAs, Br-irradiated InGaAs, Fe-ion-implanted InGaAs, and LT-InGaAs/InAlAs have been studied. Figure 4 shows a mesa-type LT-InGaAs/InAlAs structure with electrical side contacts, which improves the output power of the emitter as well as the sensitivity of the receiver [16]. One of the issues of InGaAs-related materials is low resistivity or high dark conductivity compared to GaAs materials. Detailed references and other photoconductive materials particularly used for spectroscopy applications are described in Section 4.1.

Photoconductors are used for both pulsed and CW THz sources as well as detectors, while photodiodes are more suitable for CW generation in terms of output power. In CW THz generation, two lightwaves with different wavelengths are injected onto the photoconductors or photodiodes. This technique is usually referred to as "photomixing." In contrast to the continuous evolution of photoconductors since the 1970's, studies on high-frequency photodiodes accelerated in the 1990's, mainly because of increasing demands in broadband receivers in fiber-optic communications systems [17]. There have been many approaches to enhance photodiode performances with respect to structure design, carrier transport design, and circuit design. Regarding the structure design, conventional surface-illuminated photodiodes have evolved as shown in Figure 5 [10]. In order to enhance the efficiency of the back-illuminated photodiode, a refracting facet structure was introduced to enable edge-illumination; it also contributes to ease of packaging and eases optical alignment. Other types of edge-illuminated photodiodes are waveguide structures, periodically loaded traveling-wave (TW) structures integrated with optical waveguides, and evanescently coupled TW waveguide structures. These approaches offer both high efficiency and large bandwidth.

By considering the carrier dynamics in the photodiode, several types of layer structures and materials have been proposed starting from the conventional pin photodiode (a) as illustrated in Figure 6. These are referred to as the uni-travelling-carrier photodiode (UTC-PD) (b), dual depletion pin PD (c), partially doped absorber PD (d), and modified UTC-PD, which is a composite of the UTC-PD and the dual depletion pin PD (e).

The third method to enhance the bandwidth and/or output power is a resonant operation of the back-illuminated "lumped" photodiode. This technique compensates for the internal capacitance of the photodiode, thus eliminating the constraint of CR time constant at a specific frequency. The addition of a matching element, such as a short-stub, to the photodiode was proven to increase the output power by 2-3 dB at the resonant frequency. Integration of a resonant planar antenna with the photodiode is also effective, in particular for THz regions.

Figure 7 shows a comparison of reported continuous millimeter- and THz-wave output power (detected) against operating frequency for UTC-PDs, pin-PDs, and low-temperature-grown (LT)-GaAs photomixers. The output power of UTC-PDs is about two orders of magnitude higher than those of pin-PDs, mostly due to high saturation output current. The output power decreases in proportion to f^{-4}.

To overcome the limitation of the power capacity in a single device, the power combining technique using an array of photodiodes is promising to increase the output power by one order of magnitude. There are two methods of power combining: one uses an electrical power combiner circuit,

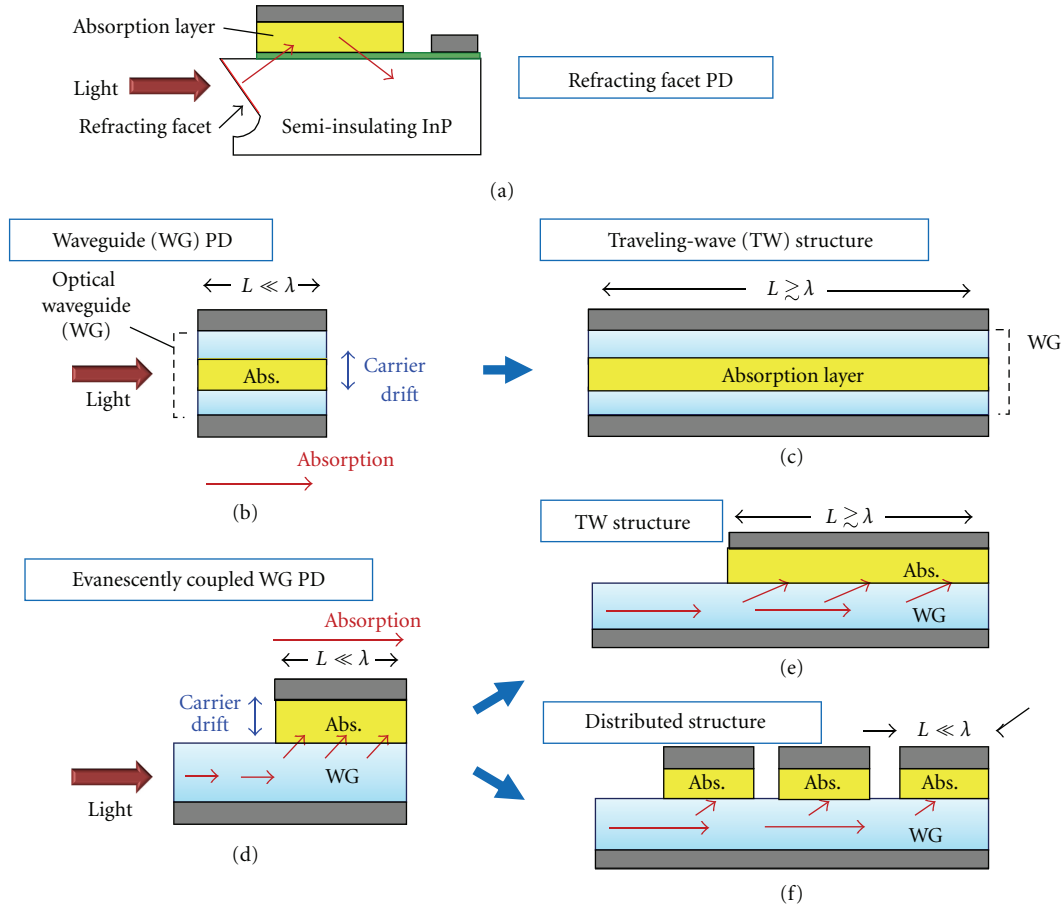

FIGURE 5: Structures of edge-illuminated photodiodes.

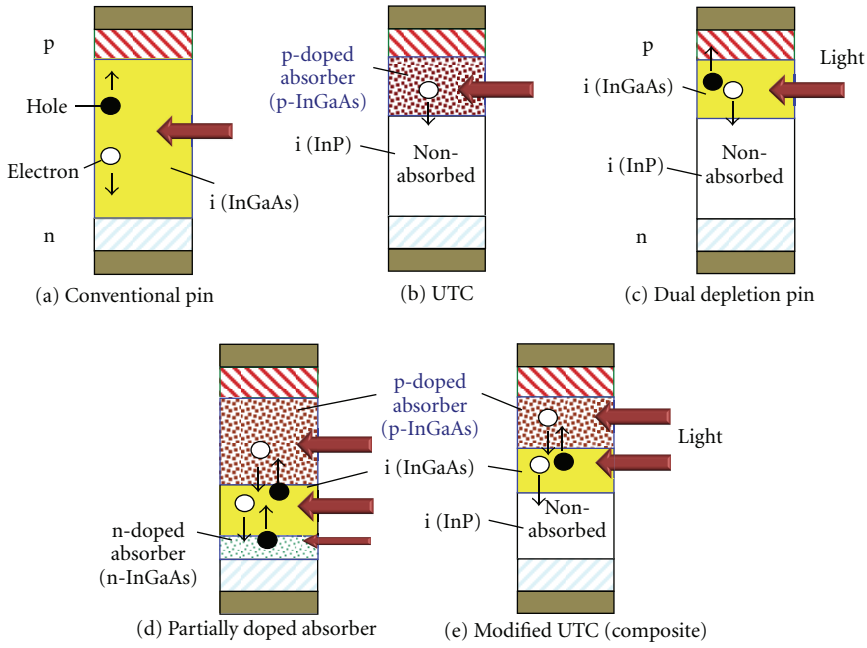

FIGURE 6: Layer structures of high-power and high-frequency photodiodes.

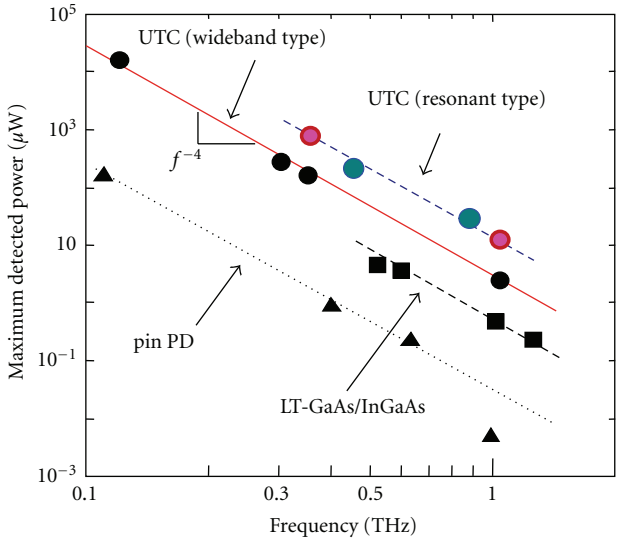

FIGURE 7: Comparison of CW output power from photodiodes and photoconductors.

and the other is based on spatial power combination using an array of antennas; both methods have been examined, as shown in Figure 8 [18, 19], achieving more than 1 mW at 300 GHz.

In addition to continuous-wave signal generation using photodiodes, there have been recently several studies on the application of photodiodes for THz heterodyne/homodyne detectors by making use of their nonlinearity [20, 21].

2.2. Low-Loss Waveguides for THz. While source and detector technologies continue to advance, considerable improvement is also needed in passive components before THz measurement and instrumentation is as economically accessible, easy to use, and high in performance as existing technology operating at lower (microwave) or higher (optical) frequencies. A large number of THz applications and instruments continue to emerge, but widespread exploitation of THz technology requires substantial improvements in both form and function. A simple example is a single-frequency source connected through a device under test to a spectrum (power spectrum) or network (S-parameters) analyzer. At microwave frequencies, precision sources are easily connected through inexpensive cables to easy-to-use analyzers. At optical frequencies, diode lasers, optical fiber, fiber-based passive and active components, and low-noise receivers provide similar efficacy. However, at THz frequencies, this simple configuration remains a research challenge involving specialized lasers, optical and THz beam alignments, and sampling delay lines. Existing technology does not easily or affordably allow the generation of a specified frequency, and passive components such as cables, connectors, couplers, filters, and circulators do not exist.

A significant first step is to develop components and systems in which THz waves are entirely confined within waveguide or transmission-line structures, rather than radiating as free-space beams as is typically done in today's systems. This has motivated considerable research on waveguide or transmission line technology for THz applications. Two broad categories of activity in THz waveguides include (1) THz "cable"—a low-loss nondispersive interconnection between various THz components or instruments over bench-top distances (>10 cm), and (2) THz on-chip interconnect—a planar interconnection between small active devices (transistors, photomixers, mixers, etc.) over on-chip distances (<1 cm) in a THz component. In what follows, we review work in both these areas. Also, since desirable solutions for these two applications differ substantially, we describe adaptation methods using mode-converter components.

Many types of waveguides have been evaluated for THz applications over the last decade including various configurations of planar, dielectric, and metallic structures. Early work with coplanar transmission lines [22] suffered from high loss (20 cm^{-1}). Conventional rectangular or circular metallic waveguide has been downsized for use at THz frequencies (e.g., [23]). While loss can be low, application is limited by difficulties in fabrication, coupling from/to THz emitters/detectors, and the highly dispersive propagation of broadband radiation used commonly in pulsed time-domain THz systems. Dispersion also limits dielectric waveguides fabricated with polyethylene [24, 25] or sapphire [26]. Very low loss (0.03 cm^{-1}) was demonstrated using the radially polarized mode supported by a bare wire [27, 28]. However, coupling to this radial mode is difficult [29], and the resulting structure lacks practical compatibility with many applications.

2.2.1. THz "Cable". For dispersion-free TEM-mode propagation, parallel-plate waveguide [30] and two-wire waveguide [31–33] offer extremely low loss (<0.01 dB/cm). Unlike a coaxial cable, both structures support a mode profile that matches well to the field emitted from typical THz sources. The strong confinement of the field between the conductors enables low bend loss [34] while the geometry can be optimized to suit a variety of objectives trading off loss for confinement. Either of these structures provides a suitable basis for low-loss guided-wave bench-top THz interconnections.

We studied the 2-wire waveguide in detail to understand loss [32] and coupling [33]. Analysis using conformal mapping shows the dependence of conductor loss on wire radius R and center-center separation D for gold wires, as shown in Figure 9. For radii greater than roughly 200 μm and separations greater than 1500 μm, conductor loss is less than 0.01 cm^{-1}. Under these conditions, the field is broadly distributed throughout the space surrounding the wires. Alternatively, for close wire spacing, the field is concentrated in a small region between the wires and loss increases.

To make a practical waveguide or cable, a suitable mechanical structure must be devised to support the parallel wires with good mechanical stability and low loss. Extending common practice in high performance microwave cables, low-density foam has been shown to provide excellent characteristics at THz frequencies. As shown in [35], rigid polymethacrylimide (PMI) foam has permittivity of

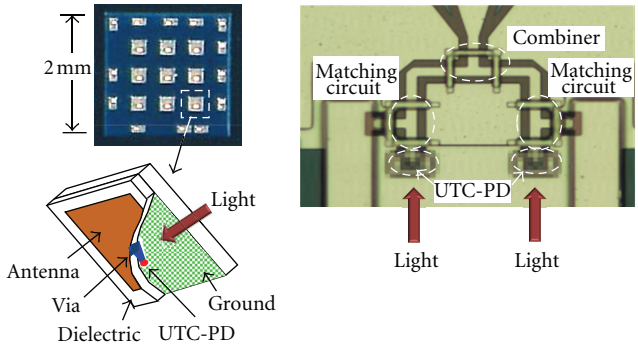

FIGURE 8: Power combining techniques with photodiode arrays by (a) spatial power combiner and (b) electrical power combiner.

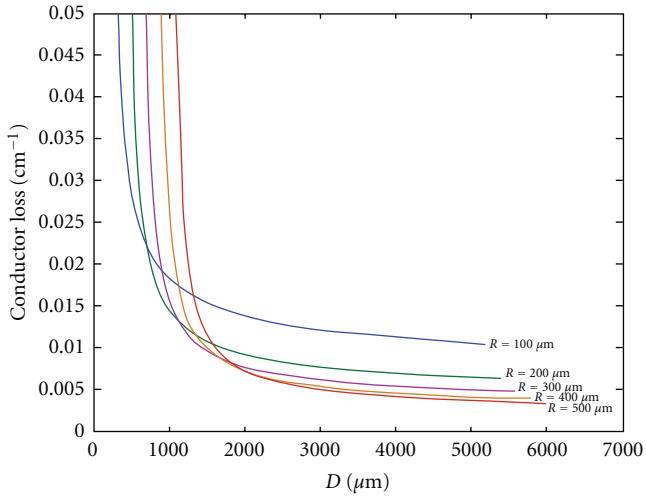

FIGURE 9: Dependence of conductor loss on wire radius R and center-center separation D for two-wire waveguide using gold wires at 1 THz.

only 1.03 and a loss tangent of <0.5%. Our recent results with a test THz "cable," formed using PMI as shown in Figure 10 to stabilize the wires, suggest that total loss as low as 0.02 cm^{-1} can be achieved at 1 THz. Dielectric loss was minimized by using periodic PMI supports over only 10% of the length of the structure.

2.2.2. THz On-Chip Interconnect. Planar structures using variants of microstrips, striplines, or coplanar lines are popular at microwave frequencies for ease of fabrication and general utility, but generally have high conductor and dielectric loss and suffer from shock-wave radiation loss [36] at higher frequencies. The latter has been reduced using suspended membrane structures [37] to prevent the propagating mode from being drawn into the substrate, but these are useful only over very short distances and are challenging to fabricate.

We have recently explored methods to reduce this radiation loss using either a symmetric cap layer or a photonic band gap structure [38]. As shown in Figure 11, we begin with a slot-line structure, which is easy to fabricate highly compatible with photoconductive THz devices and offers good heat dissipation. The basic slot-line structure (a) offers the easiest solution, but loss is high. The addition of a symmetric cap layer (b) prevents loss into the substrate, but limits access to the surface of the chip for component mounting, optical pumping, or electrical connections. Alternatively, the photonic band gap structure (c) provides a simple way to prevent this loss into the substrate, with only minor complication in the design of the substrate. However, this approach introduces frequency dependence in propagation.

These structures have been studied in detail, using conformal mapping and numerical simulation [38], providing several general conclusions. First, since the skin depth for gold at 1 THz is less than 80 nm, conductor loss becomes independent of conductor thickness for thickness greater than roughly 100 nm. Second, for slot widths greater than roughly 5 μm, conductor loss becomes independent of slot width. For thinner conductors or slots, conductor loss increases rapidly. Third, both structures can essentially eliminate radiation loss, leaving conductor loss of less than roughly 3 cm^{-1}. Adding the dielectric loss, for example using crystalline high-resistivity GaAs with loss of 0.5 cm^{-1} at 1 THz [39], gives a total loss of roughly 3.5 cm^{-1}.

2.2.3. Mode Converters. As seen in the preceding sections, the requirements and performance of transmission lines for a bench-top application differ substantially from those for on-chip interconnection. Clearly two-wire waveguide is not compatible with on-chip circuits and devices, and the loss associated with on-chip transmission lines, roughly 100 times greater than the loss for the two-wire waveguide, is unacceptable for bench-top applications. Obviously, then both technologies are needed, as is a mode converter to transition between one and the other.

Mode converters or adiabatic tapers are commonplace in optical and microwave systems. In optical systems, many papers have been published for applications in laser-to-fiber coupling, integrated optics, couplers, and photonic crystal fibers. The classic example at microwave frequencies is the

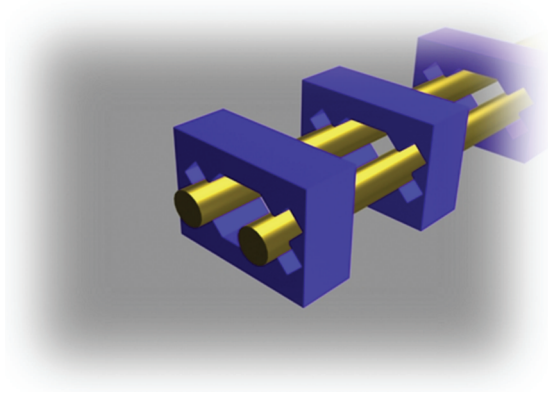

(a)

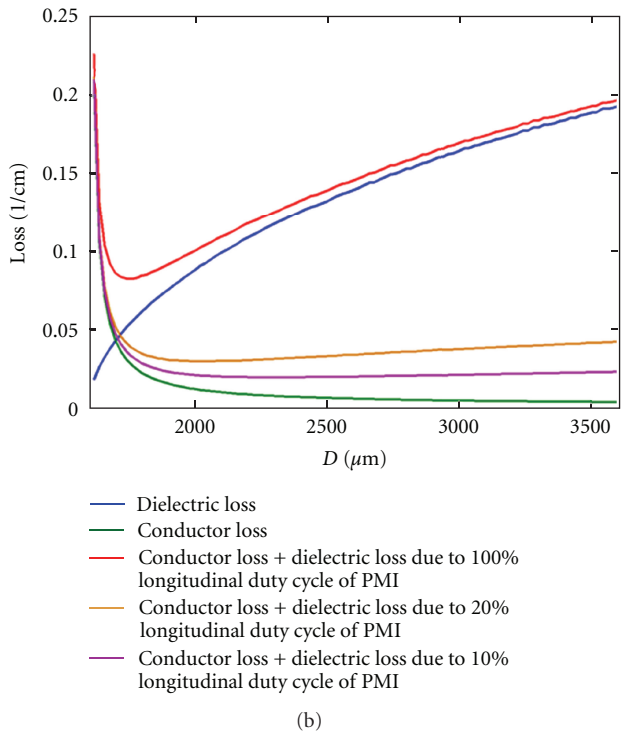

(b)

Figure 10: (a) THz cable based on two-wire waveguide with structural PMI blocks located periodically along the length. (b) Predicted performance ay 1 THz for 400 um radii wires with center-center separation D showing dielectric loss (blue), conductor loss (green), conductor loss plus dielectric loss due to 100% PMI along length (red), 20% (orange), and 10% PMI (purple).

horn antenna. The challenge is to design a structure that is simple to fabricate and provides a gradual transition between different modes while minimizing loss and reflection.

Using a mode-matching transmission-matrix approach, we studied slot-line to two-wire waveguide tapers as shown in the inset of Figure 12 [40]. Results show that this simple planar device can provide high throughput and low return loss at lengths less than 1 mm. Since conductor loss tends to be important only for the small slot widths that exist at the beginning of the taper, conductor loss tends to be small. Performance is then limited by dielectric loss. Hence it is essential to minimize the taper length and convert to a low-permittivity support structure for the two-wire waveguide as quickly as possible.

3. Communication Links

Frequency bands beyond 30 GHz are not regulated in most countries. Given the current saturation of the radio spectrum at lower bands due to thriving wireless broadband applications, there is a strong pressure toward the exploitation of new spectral regions.

3.1. Millimeter-Wave over Fiber Communications Systems. Research into millimeter-wave (mm-wave) over fiber communication systems is of interest for the support of mm-wave communications, generally, where, as was stated in Introduction, the large available spectrum can make possible ultra high-data-rate communications. The high path loss and lack of penetration through solid objects can also be made beneficial, as it can lead to well-defined cells in cellular systems. The loss experienced in electrical cables at such frequencies makes fiber transport an even more attractive proposition than at lower, microwave frequencies. However, the generation, transport, and detection of mm-wave modulated optical signals is not straightforward. Transport will be more affected by fiber dispersion as the mm-wave modulation frequency increases. Detection will require sensitive photodiodes with sufficient bandwidth and, for high-performance links, with high power-handling capability, as was shown in Figure 7, and discussed in Section 2.1. Generation requires specialized modulator configurations and/or optical generation techniques (such as optical heterodyning) due to the bandwidth limitations of optical transmitters and the need to reduce the fiber chromatic dispersion. These issues are discussed in the following subsections, followed by a brief review of mm-wave over fiber communications system architectures.

3.1.1. Fiber Transport. Although multimode fiber has been used in mm-wave over fiber systems, using techniques such as IF transmission with remote mm-wave upconversion [41], remote heterodyne detection [42] or optical frequency multiplication [43], the higher (modal) dispersion and the incompatibility of the fiber core diameter with high-speed photodiodes, have meant that most research has focussed on single-mode fiber transport. Then, it is the chromatic dispersion which poses the most significant limitation. The different phase retardations of the spectral components from the mm-wave modulation caused by the fiber dispersion results in fading of the received signal [44]; in order to overcome this, modulation or optical techniques for mm-wave generation which result in only two spectral components are necessary. Then, the different phase retardations cause phase variations of the generated mm-wave signal, but not fading. As mm-wave over fiber is an analog technique, generally large received signals are required compared to

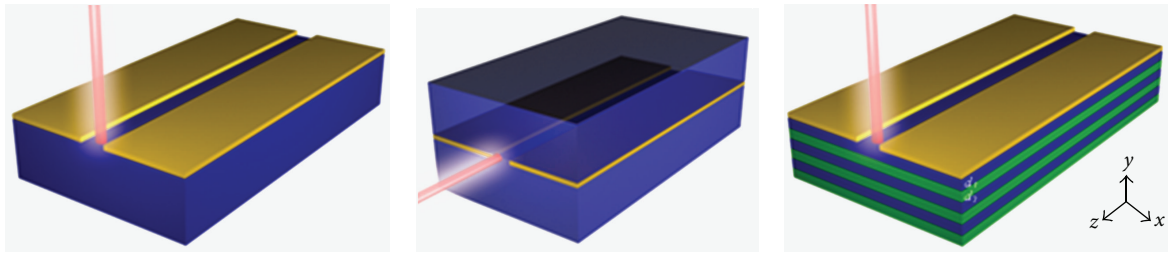

(a) (b) (c)

Figure 11: Conventional slot-line waveguide on photoconductive substrate with normal optical pump illumination, (b) edge-pumped slot-line in a homogeneous medium, and (c) slot-line on a layered substrate.

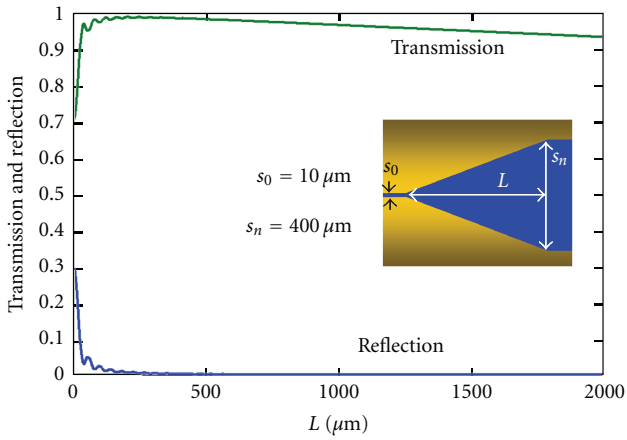

Figure 12: Transmission and reflection coefficients at 1 THz for a slot-line-based tapered structure versus L, the length of the taper, with dielectric loss = 0.5 cm^{-1}.

digital transmission; for high-performance links where optical signal levels may need to be high, or for the transport of multiple signals, fiber nonlinear effects may become significant [45].

3.1.2. Millimeter-Wave Generation. As stated in Section 3.1.1, optical generation techniques for mm-wave over fiber systems generate two optical spectral components, separated by the desired mm-wave frequency. Such schemes can be thought of as modulation-based, where the modulator setup and/or subsequent filters suppresse the undesired spectral component(s)—these are referred to as optical single-sideband (OSSB) or optical double-sideband suppressed-carrier (ODSB-SC)—or as phase-/frequency-locking based, where separate optical components are locked together. The phase/frequency locking is important because tunable optical sources such as semiconductor lasers have broad linewidth in microwave terms, and this linewidth would appear on the resultant mm-wave signal if the noise sources causing it in the individual optical spectral components were not correlated.

Simple Mach-Zehnder modulators (MZMs) can be used in mm-wave generation [46, 47]. Biasing the modulator at its null point suppresses the carrier and generates a mm-wave frequency double that of the input microwave/mm-wave frequency [46], see Figure 13(a). The method requires good control of the operating point for the carrier suppression and is limited by the bandwidth of available modulators. Frequency quadrupling is possible by biasing the MZM at its maximum transmission point and removing the carrier using a fixed optical filter [47], see Figure 13(b). Once optical filtering is considered, phase modulators may offer greater flexibility in generating the higher-order optical sidebands, which can be selected from for generating the desired mm-wave frequency [48–50] see Figure 13(c).

Conceptually, the simplest method for optically generating a mm-wave signal through the phase-locking technique is through an optical phase-locked loop which locks together two semiconductor lasers [51]. As shown in Figure 14(a), to remove the requirement for a mm-wave reference source, the locking can be done at a harmonic of the reference frequency. However, a major practical limitation is the requirement for the feedback loop delay to be much less than the timescales over which phase and frequency fluctuations occur [52]. Optical injection-locking can be performed by locking two optical sources to signals from the same reference—for example, different higher-order sidebands of the same frequency-modulated laser as shown in Figure 14(b). Here the limitation is the precise control over the laser wavelengths that is required, as locking bandwidths are typically narrow in optical terms. However, this control is possible with OPLLs, so a combination of the two techniques has been shown to be very effective [53].

Generating the optical components in a single laser source is also attractive, as the spectral lines can be locked through mechanisms such as mode-locking. Dual-mode lasers were first demonstrated for this purpose by Wake et al. (see, for example, [54]), while recently work has gone into making their behaviour more stable and predictable [55].

3.1.3. Photodetection. Small-area photodiodes can minimize capacitance and lead to possibilities for mm-wave operation, but waveguide devices enable some decoupling of the problems of collecting the photons for efficient operation and minimising the carrier transit times and device capacitance

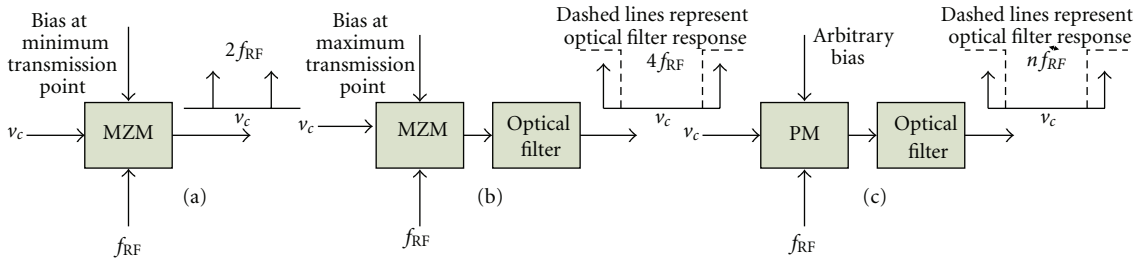

Figure 13: Millimeter-wave generation using external optical modulators: (a) frequency-doubling using a Mach-Zehnder modulator (MZM) biased at its minimum transmission point; (b) frequency-quadrupling using a MZM biased at its maximum transmission point and filtering out the optical carrier; (c) frequency n-tupling using a phase modulator and selecting appropriate sidebands.

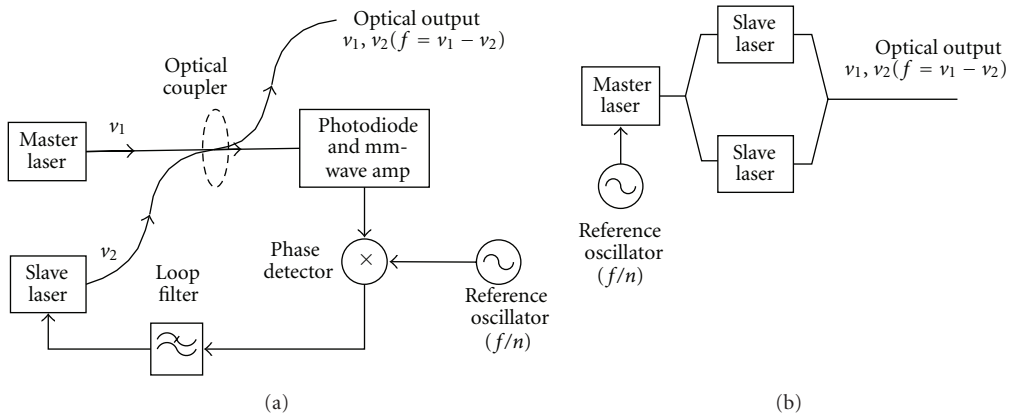

Figure 14: Millimeter-wave generation through optical heterodyning: (a) using an optical phase-locked loop (OPLL); (b) using optical sideband injection-locking.

[17]. Operation at telecommunication wavelengths with waveguide photodiodes enables the use of low-loss optical fiber for the delivery of the mm-wave signals, and such devices have been demonstrated up to over 600 GHz [56]. For mm-wave over fiber communications, however, system dynamic range is an important consideration and this is improved through operation at higher optical power levels, as will be discussed in the following subsection. Uni-traveling carrier (UTC) photodiodes, as we shown in Figure 6, have become key devices in high-speed and high-power operation.

3.1.4. Millimeter-Wave over Fiber Link Performance. As an analog link, a millimeter-wave over fiber link is characterised by gain and noise figure in its linear region, and by a dynamic range, referring to the range of signal powers that can be handled between a noise limited low end and a distortion limit at the high end. In externally modulated optical links, high optical power levels lead to higher link gains [57]; even in directly-modulated links, higher optical powers will lead to operation in a transmitter-noise-limited regime, generally resulting in lower link noise figure. It is for such reasons that UTC photodiodes have become of interest in high-performance millimetre-wave over fiber links.

Distortion, as in analog optical links generally, is mainly due to the optical transmitter—the laser or external modulator nonlinearity—although at very high optical power levels (perhaps, 10 mW and above) fiber and photodiode nonlinearity can be significant. In links where MZM-type external modulators are used to apply the data-carrying modulation to the mm-wave signal, optimization of the bias can trade off the limitations arising from distortion and noise [58].

Today, many wireless systems use higher-level, quadrature amplitude modulation (QAM) schemes to maximise the use of available bandwidth. In some cases, the QAM is applied to an orthogonal frequency-division multiplexed (OFDM) signal, which alleviates multipath and intersymbol interference effects in the wireless channel. OFDM in the optical domain may offer some resilience to fiber dispersion effects, too [59]. In general, however, these advantages must be traded against the higher peak-to-average power ratio (PAPR) obtained with OFDM and multicarrier transmission, which leads to more significant signal degradation through nonlinear effects. With QAM signals, it is common to measure performance in terms of the error vector magnitude (EVM)—a ratio of the mean error power against the mean peak signal power, measured at the outermost signal constellation point. In a noise-limited regime, at least, EVM can be directly related to signal-to-noise ratio (SNR) [60]. Different wireless systems will express performance requirements as EVM (%) for given QAM-levels; it is important to note that for radio over fiber (including mm-wave over fiber) downlink performance, it is the more stringent transmitter

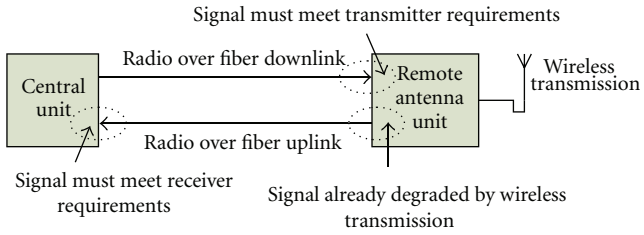

Figure 15: Radio (millimeter-wave) over fiber link performance characterization: the radio over fiber link is generally part of a larger system, and measurements must be compared to appropriate transmitter and receiver requirements.

EVM requirement that is important. This measurement against different transmitter and receiver requirements is illustrated in Figure 15. While EVM is often used to express the performance requirements against in-band noise and distortion, the optical link noise and distortion together with amplification in the antenna unit will also cause emissions out-of-band, and these must be controlled within spectral mask and adjacent channel power leakage limits.

3.1.5. Millimeter-Wave over Fiber System Architectures. For communications applications, the transport of the mm-wave signals over fiber is often necessary for connecting networks of distributed or remote antenna sites. Different fiber topologies have been proposed. For example, a star/tree topology, with space-division multiplexing (SDM) in the form of multifiber cables to distribution points, wavelength-division multiplexing (WDM), and subcarrier multiplexing (SCM) for smaller areas and individual antennas was proposed in [61]. The possible use of multimode fiber for in-building distribution was also accounted for. Ring and bus fiber topologies have also been proposed [62, 63], with the use of a secondary ring for protection against failures proposed in [64].

For the mm-wave signal transport, some proposals have examined transmission using baseband or IF signals with up-conversion to the mm-wave frequency, or downconversion from the mm-wave frequency, taking place at the remote unit [41, 65]. This has been particularly suggested for the uplink direction [65]. Experimental demonstrations of very high-bit-rate mm-wave signals over fiber have been performed [66]; those which have included a wireless link have shown the possibility for such fiber links to replace or extend point-to-point mm-wave links (e.g., for the backhaul of mobile systems) [67]. Other experiments have demonstrated the possibility of wireless local area network-type coverage over small areas using the mm-wave frequency bands [68].

3.2. THz Communications Based on Photonic Technology. Recently, there has been an increasing interest in the application of THz waves to wireless communications [69–71]. This is because frequency bands above 275 GHz have not yet been allocated to specific active services, and there is a possibility to employ extremely large bandwidths for ultrabroadband wireless communications. In particular, the 300–500-GHz range is considered to be rather realistic since enabling semiconductor electronic and photonic devices operating at this frequency range have recently started to become available. From the viewpoint of atmospheric attenuation of electromagnetic waves, 500 GHz is nearly an upper limit in "last-one-mile" applications.

In order to examine the wireless link using 300–500-GHz carrier frequencies, the use of "photonics" is practical and powerful because of large its bandwidth in the signal generation and modulation [72, 73].

Figure 16 shows a block diagram of a short-distance (~0.5 m) wireless link using a photonics-based transmitter. First, an optical THz-wave signal is generated by heterodyning the two wavelengths of light from the wavelength-tunable light sources. The optical signal is digitally modulated by the optical intensity modulator driven by the pulse pattern generator (PPG). Finally, the optical signal is converted to an electrical signal by a uni-traveling-carrier-photodiode (UTC-PD) and is emitted into free space via a horn antenna with a gain of 25 dBi. The emitted terahertz wave is well collimated by a 2-inch-diameter Teflon lens. The total antenna gain is about 40 dBi. Main features of this photonic approach are that the carrier frequency is widely tunable, and that the modulation frequency can be increased to at least 40 Gbit/s.

The receiver consists of a Schottky barrier diode (SBD) followed by a low-noise preamplifier and a limiting amplifier. The envelope detection is performed by the SBD for the ASK (OOK) modulation. The frequency dependence of the output power from the UTC-PD module is shown in Figure 17. The 3-dB bandwidth is 140 GHz (from 270 to 410 GHz). The peak output power was 110 μW at 380 GHz for a photocurrent of 10 mA with a bias voltage of 1.1 V. The output power could be further increased to over 500 μW with increasing the photocurrent up to 20 mA with responsivity of 0.22 A/W [74]. The SBD detector has almost the same bandwidth of over 100 GHz.

Figure 18 shows bit-error-rate (BER) characteristics at 12.5 Gbit/s with a carrier frequency of 300 GHz. The horizontal axis is the photocurrent of the transmitter. An error-free transmission at 12.5 Gbit/s has been achieved with 4-mA current, which corresponds to the transmitter output of around 10 μW. Currently, IF (baseband) bandwidth for demodulated signals in the receiver is as narrow as 18 GHz, which leads to the maximum bit rate of around 25 Gbit/s. Figure 18(c) shows an eye diagram of the received/demodulated signals at 24 Gbit/s. The eye is clear and open, which shows an error-free transmission.

Future challenges should address the increase of the receiver bandwidth towards 40-Gbit/s transmission and the integration of photonic components into a one-chip transmitter consisting of lasers, modulators, photodiodes, and antennas [75, 76].

4. Spectroscopy

The submillimeter-wave (Terahertz) electromagnetic spectrum hosts a wide range of complex interactions between

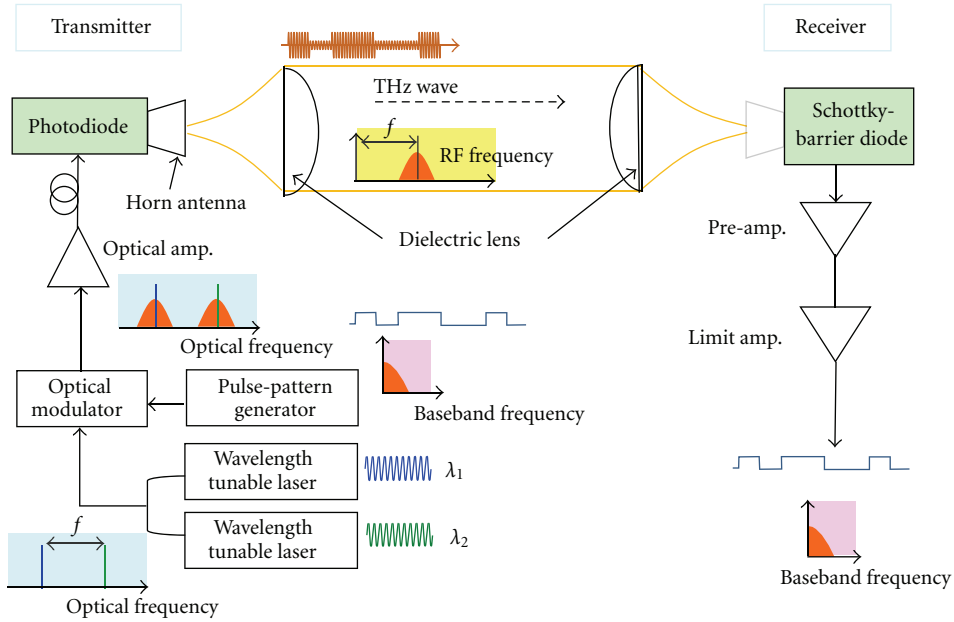

Figure 16: Schematic diagram of a 300-GHz band wireless link using photonics-based transmitter.

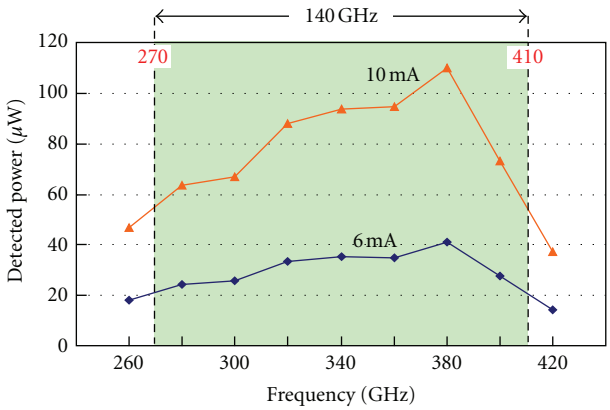

Figure 17: Typical frequency dependence of the output power from UTC-PDs.

radiation and matter that can be used to achieve innovative sensing and imaging systems. Low-energy interactions in a wide range of materials can be studied with spectroscopy in the THz range. Spectroscopic analysis in this band started with the development of Fourier Transform Infrared (FTIR) Spectroscopy in the 50 s [77]. Further developments in the last decades have resulted in alternative techniques to exploit this area of the electromagnetic spectrum.

THz spectroscopic techniques are often far superior to conventional tools for analyzing a wide variety of materials [8]. Additionally, terahertz waves are nonionizing and transparent through many materials that are opaque in visible and IR light while many other materials present characteristic spectroscopic fingerprints in this area of the spectrum. Finally, wavelengths are short enough to give adequate spatial resolution for imaging or localization of threat objects allowing spectroscopic imaging. The recent development of new sources and detectors jointly with the capability to probe fundamental physical interactions in this, previously inaccessible, spectral range has attracted considerable interest into the field of submillimeter, or THz, spectroscopy [11, 12].

Thus, THz spectroscopy has been applied to a wide range of fields with, for the moment, heterogeneous evolution to market exploitation.

(i) *Material science*. There are a wide range of optical resonances in molecular crystals within the THz band given by the complicated interplay between intra- and intermolecular forces. In recent years, the spectroscopic analysis of polyatomic crystals, and especially crystals of organic molecules, have attracted considerable interest for chemical recognition [78]. THz spectroscopy has been applied also to the study of low-energy carrier dynamics in semiconductors, quantum dots, superconductors, and strongly correlated electron materials as well as conductivity studies in electronic materials [12]. Finally, liquids have been also extensively studied with THz spectroscopy [11]. In this case, THz absorption spectrum of a liquid is dominated by relaxation of either permanent dipoles in polar liquids (e.g., water or ethanol) or collision induced dipole moments in nonpolar liquids (e.g., benzene or toluene). Since most chemical reactions of importance in biology occur in an aqueous environment, a considerable percentage of the studies on the application of THz spectroscopy to liquids have been devoted to water and aqueous solutions of salts, sugars, and lower alcohols [11, 79].

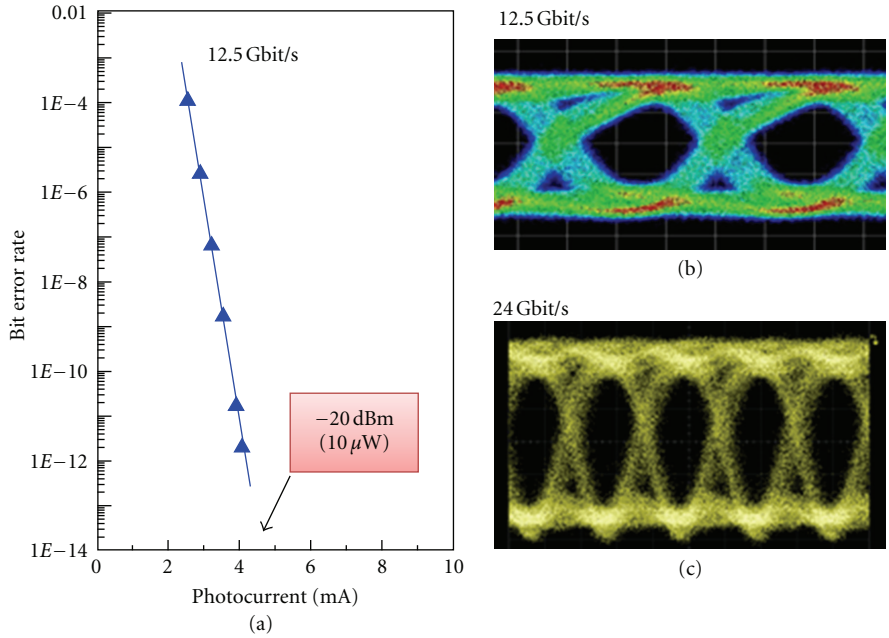

Figure 18: (a) Bit error rate characteristics of the wireless link at 12.5 Gbit/s. Eye diagrams at (b) 12.5 Gbit/s and (c) 24 Gbit/s.

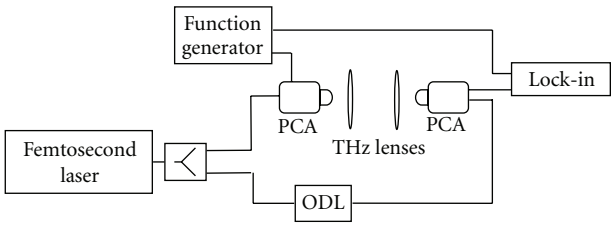

Figure 19: Block diagram of a generic fiber-based THz-TDS system.

(ii) *Biological and pharmaceutical substances*. The capability of THz spectroscopy to observe intermolecular vibrations in some chemicals and organic molecules has led to its application to biomolecules, medicines, cancer tissue, DNA, proteins, and bacteria [8, 80, 81]. Another application is for polymorph classification in pharmacology [82]. There are substances that can be clearly identified from their THz-absorption spectra whereas FTIR measurements donot provide positive recognition. THz spectroscopy has also been applied for clinical diagnosis, in particular for discrimination between cancerous cells (basal cell carcinoma) and normal tissue [83]. However, the high cost of these systems has prevented practical clinical application of this approach.

(iii) *Safety and security*. The capability for contactless chemical identification of THz waves jointly with the discovery of THz signatures of common explosives [84] led to the study of THz imaging and spectroscopy for detection of concealed explosives, drugs, and weapons. In particular, a wide set of security applications have been analyzed ranging from THz cameras, detection of chemical and biological weapons, to archway body scanners for security checkpoints at airports, customs and even stand-off detection of explosives, improvised-explosive devices. Although several demonstrations of mail and luggage inspection have been successful [85, 86], the relatively weak and broad explosive signatures are regularly masked by the combined effects of atmospheric vapor absorption, barrier attenuation, and scattering from both clothing and the own explosive, making the practical deployment of remote through-barrier THz spectroscopic explosive detection systems very difficult to implement [87].

(iv) *Industrial monitoring*. The THz spectrum can be used to monitor a wide range of industrial processes including polymeric compounding [88], quality control of plastic weld joints [89], moisture content in polymers [90], plastic fiber orientation [91], paper thickness and moisture content [92], and monitoring of industrial pollution [93], to cite some of them. Demonstrators have been presented, but technology improvements in terms of emitted power, scanning speed, and cost are needed to take advantage of the information in the THz domain while offering a competitive product.

Other applications include art conservation [94], detection of foreign bodies in food [95], pollutant and pesticide residue monitoring in food [96], and, last but not least, astronomy, the first field where far-infrared technology was developed [97, 98].

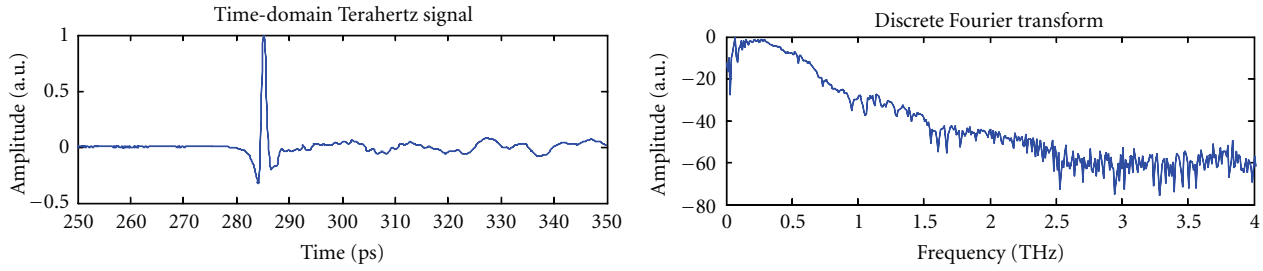

(a) (b)

Figure 20: (a) Fiber-based THz-TDS temporal signal, (b) Fourier transform of (a).

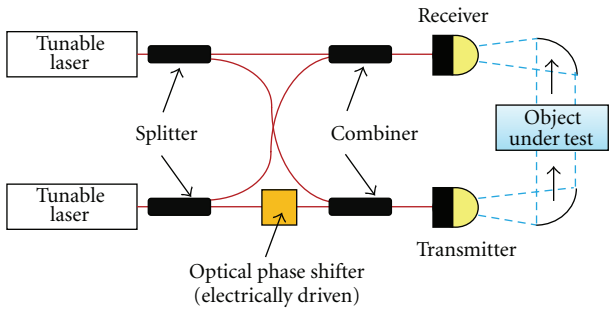

Figure 21: Schematic diagram of frequency domain spectroscopy (FDS) system using an optical phase shifter.

The main limitations to the wide deployment of THz spectroscopy in practical applications are related to current performance of THz technology, bulkiness of the instruments, and high cost. To overcome these restrictions, fiber optic technology can offer an interesting implementation in comparison to conventional bulk optics systems usually employed in THz spectroscopy.

4.1. Fiber-Optic THz Time Domain Spectroscopy. Sensing in the THz regime can be done using Fourier transform infrared (FTIR) spectroscopy. However, in the late 80s, an alternative method was proposed based on the excitation with femtosecond pulses of photoconductive dipole antennas to generate short pulses of THz radiation to probe materials [99]. This technique is known as THz Time-Domain Spectroscopy (THz-TDS). Unlike FTIR which is sensitive only to amplitude, THz-TDS can detect changes induced by the sample in both amplitude and phase, providing more information since real and imaginary parts of the optical constants are deduced simultaneously without using Kramers-Kronig analysis. Additionally, THz-TDS avoids the effect of background thermal radiation since THz waves are detected coherently unlike FTIR.

THz-TDS is based on producing terahertz energy using photoconductive switches or antennas (PCA) [7, 100]. A PCA is an electrical switch exploiting the increase in electrical conductivity of semiconductors and insulators when they are exposed to light [101]. Several photoconductive materials have been tested for PCA: low-temperature grown gallium arsenide (LT-GaAs), radiation-damaged silicon-on-sapphire (RD-SOS), chromium-doped gallium arsenide (Cr-GaAs), indium phosphide (InP), and amorphous silicon. Among these LT-GaAs is probably the most common. The physical mechanism begins with an ultrafast laser pulse (with photon energy larger than the bandgap of the material), which creates electron-hole pairs in the photoconductor. The free carriers then accelerate in the static bias field to form a transient photocurrent, and the fast, time-varying current radiates electromagnetic waves [100]. To provide photons with enough energy, pulsed sources at 780–820 nm as Ti:Sapphire lasers are regularly used to match the bandgap of LT-GaAs. Typical optical-to-terahertz conversion efficiencies are below 10^{-5}. Even so, photoconductive emitters are capable of providing relatively large average THz power in comparison with other approaches with level powers up to 40 μW and bandwidths usually up to 4 THz [102] although recently has been demonstrated that by removing all absorbing elements in the THz beam path and using the shortest possible laser pulses (10 fs), photoconductive detection of frequencies approaching 100 THz has been reported [103].

Recently, other materials with smaller bandgaps than LT-GaAs have been proposed as photoconductive material. This allows the replacement of expensive and bulky Ti:Sapphire sources by cost-effective telecom 1550 nm sources. These materials include LT-InGaAs [104], LT-GaAsSb [105], ion-implanted InGaAs [106], and superlattice structures with LT-InGaAs/InAlAs [16, 107].

These new materials allow the implementation of fiber-optic THz-TDS systems [107]. These use a femtosecond fiber laser at telecom wavelengths (1550 nm) instead of a Ti:Sapphire (800 nm) which can reduce the cost of the photonic source between half and less than a third of the original budget. Figure 19 shows a setup for a fiber-based THz-TDS system. A fiber pulse source is used to generate 100 fs pulses which are split into two branches which fed two fiber-pigtailed PCAs. An optical delay line (ODL) is used to map THz traces, as shown in Figure 20. Fiber-based THz-TDS systems offer higher stability as well as reduced size and power consumption, and there are a wide range of mature, low-cost components developed for the optical communications market. Additionally, fiber-optic components

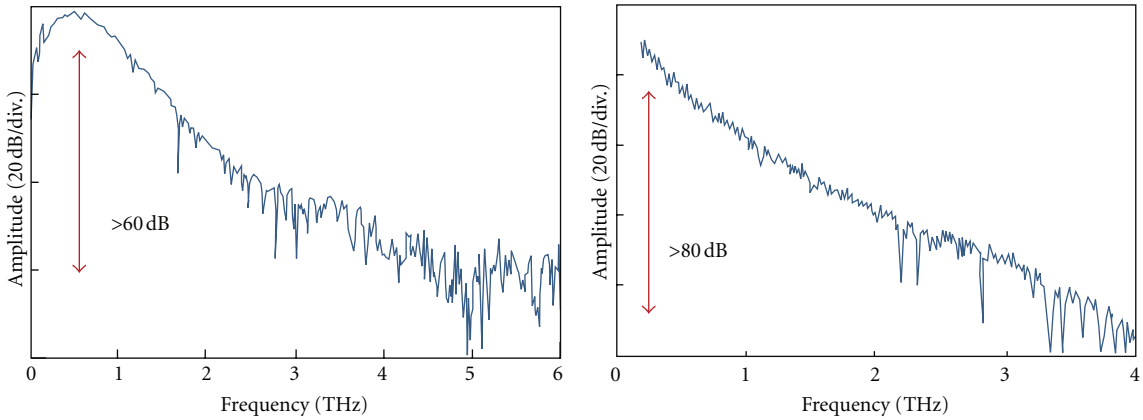

Figure 22: Comparison of typical spectral characteristics for (a) TDS and (b) FDS.

allow the implementation of compact, low-weigh, and robust THz-TDS systems. Finally, telecom wavelengths and fiber-illuminated antennas allow the implementation of remote delivery for THz systems with small emitter and receiver heads and even sharing of a single optical source by several remote emitter/receiver heads to allow further cost saving [108].

4.2. Frequency Domain Spectroscopy. Recently, THz spectroscopy systems based on CW technology, which use monochromatic sources with an accurate frequency control capability, have attracted great interest [76, 109–113]. The CW source-based systems, referred to as frequency-domain spectroscopy (FDS), provide higher signal-to-noise ratio (SNR) and spectral resolution. When the frequency band of interest is targeted for the specific absorption line of the objects being tested, FDS systems with the selected frequency-scan length and resolution are more practical in terms of data acquisition time as well as system cost.

A THz-FDS system with photonic emitters and detectors is frequently called a homodyne system, and its configuration is the same as that of the THz-TDS system except for the optical signal source. The optical delay line is fixed after being adjusted to maximize the interference signal in case of the homodyne detection. In addition, the optical delay line can be replaced by the optical phase shifter such as electrooptic phase modulators and piezo-electric phase shifters as shown in Figure 21 [114, 115]. This method not only leads to the increase in the speed of delay change, but also enables an accurate phase measurement.

Like THz-TDS systems, THz-FDS systems are commercially available, which employ nonlinear crystals [116], photoconductive antennas (PCAs) [117–119], photodiodes [118] for THz generators, and electrooptic (EO) crystals [116], and photoconductive antennas (PCAs) [117–119] for THz detectors.

Figure 22 shows typical frequency spectra obtained with the fiber-optic TDS and FDS systems, respectively, which were reported by the Fraunhofer Heinrich Hertz Institute [120]. The FDS system offers >80 dB dynamic range, which is higher than that of the fiber-optic TDS.

5. Conclusion

Different photonic technologies and applications based on the millimeter- and submillimeter-wave bands have been discussed in this overview paper. The key elements for the photonic generation and detection of high frequency signals (photodiodes and photoconductors) have been analyzed and a comparison has been provided. Recent advances in guided-wave techniques for THz systems have also been reviewed. The main conclusions are that for bench-top interconnection applications, the combination of dielectric loss and conductor loss forces the use of large conductors and conductor separations relative to those required for an on-chip application. It can be found that the two-wire waveguide offers the best combination of performance and practicality for bench-top terahertz interconnections in guided-wave systems. For on-chip applications, where a substrate is deemed essential and dimensions are typically less than a millimeter, we find that the slot line offers high performance, if suitable methods are employed to eliminate power loss into the substrate. Finally, adiabatic mode-converting tapers have been reviewed showing that these can be fabricated easily and with low loss. This work suggests that guided-wave terahertz systems may soon begin to displace the free-space systems in routine use today and enable new classes of terahertz applications and instruments with better performance and utility.

Two applications for the application of photonic technology to the millimeter and submillimeter-wave bands have been reviewed. First, it has been shown how different photonic technologies can be applied to generate and distribute signals in these bands to implement high-bit rate access network which will foster the deployment of new high bit-rate applications. Future challenges should address the increase of the receiver bandwidth towards 40-Gbit/s transmission and the integration of photonic components

into a one-chip transmitter consisting of lasers, modulators, photodiodes, and antennas. Additionally, the application of photonic technology to spectroscopic sensing has been also reviewed showing that both time- and frequency-domain spectroscopy systems can benefit from fiber-optic implementation easing the application of sensing in these spectral regions.

To summarize, the development of new components and architectures is paving the way to the deployment of applications in fields such as communications and sensing that offer new functionalities and capabilities. These technologies are playing a significant part in the increasing utilization of currently unproductive spectral regions.

Acknowledgments

B. Vidal would like to thank the Spanish Ministerio de Economia y Competitividad for its support through Project TEC2009-08078. T. Nagatsuma would like to acknowledge the financial support provided by the Ministry of Education, Science, Sports and Culture, Grant-in-Aid for Scientific Research (A) 23246067, 2011 and the JST-ANR WITH program.

References

[1] G. P. Agrawal, *Fiber Optic Communication Systems*, John Wiley & Sons, New York, NY, USA, 2010.

[2] A. J. Seeds, "Microwave photonics," *IEEE Transactions on Microwave Theory and Techniques*, vol. 50, no. 3, pp. 877–887, 2002.

[3] J. Capmany and D. Novak, "Microwave photonics combines two worlds," *Nature Photonics*, vol. 1, no. 6, pp. 319–330, 2007.

[4] R. C. Williamson and R. D. Esman, "RF photonics," *Journal of Lightwave Technology*, vol. 26, no. 9, pp. 1145–1153, 2008.

[5] J. Yao, "Microwave photonics," *Journal of Lightwave Technology*, vol. 27, no. 3, pp. 314–335, 2009.

[6] T. Berceli and P. R. Herczfeld, "Microwave photonics—a historical perspective," *IEEE Transactions on Microwave Theory and Techniques*, vol. 58, no. 11, pp. 2992–3000, 2010.

[7] P. H. Siegel, "Terahertz technology," *IEEE Transactions on Microwave Theory and Techniques*, vol. 50, no. 3, pp. 910–928, 2002.

[8] M. Tonouchi, "Cutting-edge terahertz technology," *Nature Photonics*, vol. 1, no. 2, pp. 97–105, 2007.

[9] B. Ferguson and X. C. Zhang, "Materials for terahertz science and technology," *Nature Materials*, vol. 1, no. 1, pp. 26–33, 2002.

[10] T. Nagatsuma, "Generating millimeter and terahertz waves," *IEEE Microwave Magazine*, vol. 10, no. 4, pp. 64–74, 2009.

[11] P. U. Jepsen, D. G. Cooke, and M. Koch, "Terahertz spectroscopy and imaging—modern techniques and applications," *Laser and Photonics Reviews*, vol. 5, no. 1, pp. 124–166, 2011.

[12] S. L. Dexheimer, *Terahertz Spectroscopy*, CRC Press, New York, NY, USA, 2008.

[13] K. L. Yeh, M. C. Hoffmann, J. Hebling, and K. A. Nelson, "Generation of 10 μJ ultrashort terahertz pulses by optical rectification," *Applied Physics Letters*, vol. 90, no. 17, Article ID 171121, 3 pages, 2007.

[14] A. G. Stepanov, S. Henin, Y. Petit, L. Bonacina, J. Kasparian, and J. P. Wolf, "Mobile source of high-energy single-cycle terahertz pulses," *Applied Physics B*, vol. 101, no. 1-2, pp. 11–14, 2010.

[15] E. R. Brown, "Advancements in photomixing and photoconductive switching for THz spectroscopy and imaging," in *4th Terahertz Technology and Applications*, vol. 7938 of *Proceedings of SPIE*, San Francisco, Calif, USA, January 2011.

[16] H. Roehle, R. J. B. Dietz, H. J. Hensel et al., "Next generation 1.5 μm terahertz antennas: mesa-structuring of InGaAs/InAlAs photoconductive layers," *Optics Express*, vol. 18, no. 3, pp. 2296–2301, 2010.

[17] K. Kato, "Ultrawide-B and/high-frequency photodetectors," *IEEE Transactions on Microwave Theory and Techniques*, vol. 47, no. 7, pp. 1265–1281, 1999.

[18] N. Shimizu and T. Nagatsuma, "Photodiode-integrated microstrip antenna array for subterahertz radiation," *IEEE Photonics Technology Letters*, vol. 18, no. 6, pp. 743–745, 2006.

[19] H. J. Song, K. Ajito, Y. Muramoto, A. Wakatsuki, T. Nagatsuma, and N. Kukutsu, "Uni-travelling-carrier photodiode module generating 300 GHz power greater than 1 mW," *IEEE Microwave and Wireless Components Letters*, vol. 22, no. 7, pp. 363–365, 2012.

[20] T. Nagatsuma, A. Kaino, S. Hisatake et al., "Continuous-wave terahertz spectroscopy system based on photodiodes," *PIERS Online*, vol. 6, no. 4, pp. 390–394, 2010.

[21] E. Rouvalis, M. J. Fice, C. C. Renaud, and A. J. Seeds, "Millimeter-wave optoelectronic mixers based on uni-traveling carrier photodiodes," *IEEE Transactions on Microwave Theory and Techniques*, vol. 60, no. 3, pp. 686–691, 2012.

[22] M. Y. Frankel, S. Gupta, J. A. Valdmanis, and G. A. Mourou, "Terahertz attenuation and dispersion characteristics of coplanar transmission lines," *IEEE Transactions on Microwave Theory and Techniques*, vol. 39, no. 6, pp. 910–916, 1991.

[23] G. Gallot, S. P. Jamison, R. W. McGowan, and D. Grischkowsky, "Terahertz waveguides," *Journal of the Optical Society of America B*, vol. 17, no. 5, pp. 851–863, 2000.

[24] R. Mendis and D. Grischkowsky, "Plastic ribbon THz waveguides," *Journal of Applied Physics*, vol. 88, no. 7, pp. 4449–4451, 2000.

[25] L. J. Chen, H. W. Chen, T. F. Kao, J. Y. Lu, and C. K. Sun, "Low-loss subwavelength plastic fiber for terahertz waveguiding," *Optics Letters*, vol. 31, no. 3, pp. 308–310, 2006.

[26] S. P. Jamison, R. W. McGowan, and D. Grischkowsky, "Single-mode waveguide propagation and reshaping of sub-ps terahertz pulses in sapphire fibers," *Applied Physics Letters*, vol. 76, no. 15, pp. 1987–1989, 2000.

[27] K. Wang and D. M. Mittleman, "Metal wires for terahertz wave guiding," *Nature*, vol. 432, no. 7015, pp. 376–379, 2004.

[28] T. I. Jeon, J. Zhang, and D. Grischkowsky, "THz Sommerfeld wave propagation on a single metal wire," *Applied Physics Letters*, vol. 86, no. 16, Article ID 161904, 3 pages, 2005.

[29] J. A. Deibel, K. Wang, M. D. Escarra, and D. M. Mittleman, "Enhanced coupling of terahertz radiation to cylindrical wire waveguides," *Optics Express*, vol. 14, no. 1, pp. 279–290, 2006.

[30] R. Mendis and D. M. Mittleman, "Multifaceted terahertz applications of parallel-plate waveguide: TE1 mode," *Electronics Letters*, vol. 46, pp. 40–44, 2010.

[31] M. K. Mbonye, V. Astley, W. L. Chan, J. A. Deibel, and D. M. Mittleman, "A terahertz dual wire waveguide," in *Proceedings of the Lasers and Electro-Optics Conference, Optical Society of America*, p. CThLL1, Baltimore, Mary, USA, 2007.

[32] H. Pahlevaninezhad, T. E. Darcie, and B. Heshmat, "Two-wire waveguide for terahertz," *Optics Express*, vol. 18, no. 7, pp. 7415–7420, 2010.

[33] H. Pahlevaninezhad and T. E. Darcie, "Coupling of terahertz waves to a two-wire waveguide," *Optics Express*, vol. 18, no. 22, pp. 22614–22624, 2010.

[34] M. Mbonye, R. Mendis, and D. M. Mittleman, "A terahertz two-wire waveguide with low bending loss," *Applied Physics Letters*, vol. 95, no. 23, Article ID 233506, 3 pages, 2009.

[35] C. Roman, O. Ichim, L. Sarger, V. Vigneras, and P. Mounaix, "Terahertz dielectric characterisation of polymethacrylimide rigid foam: the perfect sheer plate?" *Electronics Letters*, vol. 40, no. 19, pp. 1167–1169, 2004.

[36] C. Fattinger and D. Grischkowsky, "Observation of electromagnetic shock waves from propagating surface-dipole distributions," *Physical Review Letters*, vol. 62, no. 25, pp. 2961–2964, 1989.

[37] P. H. Siegel, R. P. Smith, M. C. Gaidis, and S. C. Martin, "2.5-THz GaAs monolithic membrane-diode mixer," *IEEE Transactions on Microwave Theory and Techniques*, vol. 47, no. 5, pp. 596–604, 1999.

[38] H. Pahlevaninezhad, B. Heshmat, and T. E. Darcie, "Efficient terahertz slot-line waveguides," *Optics Express* , vol. 19, no. 26, pp. B47–B55, 2011.

[39] D. Grischkowsky, S. Keiding, M. van Exter, and C. Fattinger, "Far-infrared time-domain spectroscopy with terahertz beams of dielectrics and semiconductors," *Journal of Optical Society of America B*, vol. 7, no. 10, pp. 2006–2015, 1990.

[40] H. Pahlevaninezhad, *Design and implementation of efficient terahertz waveguides [Ph.D. thesis]*, 2012.

[41] C. Loyez, C. Lethien, R. Kassi et al., "Subcarrier radio signal transmission over multimode fibre for 60 GHz WLAN using a phase noise cancellation technique," *Electronics Letters*, vol. 41, no. 2, pp. 91–92, 2005.

[42] A. Nkansah, A. Das, N. J. Gomes, and P. Shen, "Multilevel modulated signal transmission over serial single-mode and multimode fiber links using vertical-cavity surface-emitting lasers for millimeter-wave wireless communications," *IEEE Transactions on Microwave Theory and Techniques*, vol. 55, no. 6, pp. 1219–1227, 2007.

[43] M. G. Larrodé and A. M. J. Koonen, "Theoretical and experimental demonstration of OFM robustness against modal dispersion impairments in radio over multimode fiber links," *Journal of Lightwave Technology*, vol. 26, no. 12, pp. 1722–1728, 2008.

[44] U. Gliese, S. Norskov, and T. N. Nielsen, "Chromatic dispersion in fiber-optic microwave and millimeter-wave links," *IEEE Transactions on Microwave Theory and Techniques*, vol. 44, no. 10, pp. 1716–1724, 1996.

[45] G. P. Agrawal, *Nonlinear Fiber Optics*, Academic Press, New York, NY, USA.

[46] J. J. O'Reilly, P. M. Lane, R. Heidemann, and R. Hofstetter, "Optical generation of very narrow linewidth millimetre wave signals," *Electronics Letters*, vol. 28, no. 25, pp. 2309–2311, 1992.

[47] G. Qi, J. Yao, J. Seregelyi, C. Bélisle, and S. Paquet, "Generation and distribution of a wide-band continuously tunable millimeter-wave signal with an optical external modulation technique," *IEEE Transactions on Microwave Theory and Techniques*, vol. 53, no. 10, pp. 3090–3097, 2005.

[48] P. Shen, N. J. Gomes, P. A. Davies, W. P. Shillue, P. G. Huggard, and B. N. Ellison, "High-purity millimeter-wave photonic local oscillator generation and delivery," in *Proceedings of the International Microwave Photonics Topical Meeting (WP'03)*, pp. 189–192, Budapest, Hungary.

[49] G. Qi, J. Yao, J. Seregelyi, C. Bélisle, and S. Paquet, "Optical generation and distribution of continuously tunable millimeter-wave signals using an optical phase modulator," *Journal of Lightwave Technology*, vol. 23, no. 9, pp. 2687–2695, 2005.

[50] B. Vidal, P. G. Huggard, B. N. Ellison, and N. J. Gomes, "Optoelectronic generation of W-band millimetre-wave signals using Brillouin amplification," *Electronics Letters*, vol. 46, no. 21, pp. 1449–1450, 2010.

[51] L. Goldberg, H. F. Taylor, J. F. Weller, and D. M. Bloom, "Microwave signal generation with injection locked laser diodes," *Electronics Letters*, vol. 19, no. 13, pp. 491–493, 1983.

[52] R. T. Ramos and A. J. Seeds, "Delay, linewidth and bandwidth limitations in optical phase-locked loop design," *Electronics Letters*, vol. 26, no. 6, pp. 389–391, 1990.

[53] A. C. Bordonalli, C. Walton, and A. J. Seeds, "High-performance phase locking of wide line width semiconductor lasers by combined use of optical injection locking and optical phase-lock loop," *Journal of Lightwave Technology*, vol. 17, no. 2, pp. 328–342, 1999.

[54] D. Wake, C. R. Liana, and P. A. Davies, "Optical generation of millimeter-wave signals for fiber-radio systems using a dual-mode DFB semiconductor laser," *IEEE Transactions on Microwave Theory and Techniques*, vol. 43, no. 9, pp. 2270–2276, 1995.

[55] F. van Dijk, A. Accard. Enard, O. Drisse, D. Make, and F. Lelarge, "Monolithic dual wavelength DFB lasers for narrow linewidth heterodyne beat-note generation," in *Proceedings of the International Topical Meeting on Microwave Photonics (MWP'11)*, pp. 73–76, Singapore, October 2011.

[56] P. G. Huggard, B. N. Ellison, P. Shen et al., "Generation of millimetre and sub-millimetre waves by photomixing in 1.55 μm wavelength photodiode," *Electronics Letters*, vol. 38, no. 7, pp. 327–328, 2002.

[57] C. H. Cox III, G. E. Betts, and L. M. Johnson, "Analytic and experimental comparison of direct and external modulation in analog fiber-optic links," *IEEE Transactions on Microwave Theory and Techniques*, vol. 38, no. 5, pp. 501–509, 1990.

[58] M. L. Farwell, W. S. C. Chang, and D. R. Huber, "Increased linear dynamic range by low biasing the Mach-Zehnder modulator," *IEEE Photonics Technology Letters*, vol. 5, no. 7, pp. 779–782, 1993.

[59] J. Armstrong, "OFDM for optical communications," *Journal of Lightwave Technology*, vol. 27, pp. 189–204, 2009.

[60] H. Arslan and H. A. Mahmoud, "Error vector magnitude to SNR conversion for nondata-aided receivers," *IEEE Transactions on Wireless Communications*, vol. 8, no. 5, pp. 2694–2704, 2009.

[61] A. Nkansah, A. Das, N. J. Gomes, P. Shen, and D. Wake, "VCSEL-based single-mode and multimode fiber star/tree distribution network for millimeter-wave wireless systems," in *Proceedings of the International Topical Meeting on Microwave Photonics (MWP'06)*, pp. 1–4, Grenoble, France, October 2006.

[62] C. Lim, A. Nirmalathas, D. Novak, and R. B. Waterhouse, "Capacity analysis and optimum channel allocations for a WDM ring fibre-radio backbone incorporating wavelength interleaving with a sectorized antenna interface," in *Proceedings of the International Topitcal Meeting on Microwave Photonics (MWP'02)*, pp. 371–374, November 2002.

[63] X. Zhang, B. Liu, J. Yao, and R. Kashyap, "A novel millimeter-wave-band radio-over-fiber system with dense

wavelength-division multiplexing bus architecture," *IEEE Transactions on Microwave Theory and Techniques*, vol. 54, no. 2, pp. 929–936, 2006.

[64] W. P. Lin, "A robust fiber-radio architecture for wavelength-division-multiplexing ring-access networks," *Journal of Lightwave Technology*, vol. 23, no. 9, pp. 2610–2620, 2005.

[65] Z. Jia, J. Yu, G. Ellinas, and G. K. Chang, "Key enabling technologies for optical wireless networks: optical millimeter-wave generation, wavelength reuse, and architecture," *Journal of Lightwave Technology*, vol. 25, no. 11, pp. 3452–3471, 2007.

[66] R. Sambaraju, J. Herrera, J. Marti et al., "Up to 40 Gb/s wireless signal generation and demodulation in 75–110 GHz band using photonic techniques," in *Proceedings of the IEEE International Topical Meeting on Microwave Photonics (MWP'10)*, pp. 1–4, Montreal, Canada, October 2010.

[67] M. Weiss, A. Stohr, F. Lecoche, and B. Charbonnier, "27 Gbit/s photonic wireless 60 GHz transmission system using 16-QAM OFDM," in *Proceedings of the International Topical Meeting on Microwave Photonics (MWP'09)*, Valencia, Spain, October 2009.

[68] J. James, P. Shen, A. Nkansah, X. Liang, and N. J. Gomes, "Nonlinearity and noise effects in multi-level signal millimeter-wave over fiber transmission using single and dual wavelength modulation," *IEEE Transactions on Microwave Theory and Techniques*, vol. 58, no. 11, pp. 3189–3198, 2010.

[69] J. Federici and L. Moeller, "Review of terahertz and subterahertz wireless communications," *Journal of Applied Physics*, vol. 107, no. 11, Article ID 111101, 22 pages, 2010.

[70] T. Kleine-Ostmann and T. Nagatsuma, "A review on terahertz communications research," *Journal of Infrared, Millimeter, and Terahertz Waves*, vol. 32, no. 2, pp. 143–171, 2011.

[71] H. J. Song and T. Nagatsuma, "Present and future of terahertz communications," *IEEE Trans. Terahertz Science and Technology*, vol. 1, no. 1, pp. 256–264, 2011.

[72] T. Nagatsuma, H. J. Song, Y. Fujimoto et al., "Giga-bit wireless link using 300–400 GHz bands," in *Proceedings of the IEEE International Topical Meeting on Microwave Photonics (MWP'09)*, Valencia, Spain, October 2009.

[73] H. J. Song, K. Ajito, A. Wakatsuki et al., "Terahertz wireless communication link at 300 GHz," in *PRoceedings of the IEEE International Topical Meeting on Microwave Photonics (MWP'10)*, pp. 42–45, Montreal, Canada, October 2010.

[74] A. Wakatsuki, T. Furuta, Y. Muramoto, T. Yoshimatsu, and H. Ito, "High-power and broadband sub-terahertz wave generation using a J-band photomixer module with rectangular-waveguide output port," in *Proceedings of the 33rd International Conference on Infrared and Millimeter Waves and the 16th International Conference on Terahertz Electronics, 2008, IRMMW-THz 2008*, pp. 1–2, Pasadena, Calif, USA, September 2008.

[75] A. J. Seeds, M. J. Fice, F. Pozzi et al., "Photonic-enabled microwave and terahertz communication systems," in *Proceedings of the Optical Fiber Communication (OFC'09)*, pp. 1–3, March 2009, OTuE6.

[76] M. J. Fice, E. Rouvalis, L. Ponnampalam, C. C. Renaud, and A. J. Seeds, "Telecommunications technology-based terahertz sources," *Electronics Letters*, vol. 46, no. 26, pp. s28–s31, 2010.

[77] K. D. M. Möller and W. G. Rothschild, *Far-Infrared Spectroscopy*, John Wiley & Sons, NewYork, NY, USA, 1971.

[78] B. Fischer, M. Hoffmann, H. Helm, G. Modjesch, and P. U. Jepsen, "Chemical recognition in terahertz time-domain spectroscopy and imaging," *Semiconductor Science and Technology*, vol. 20, no. 7, pp. S246–S253, 2005.

[79] J. T. Kindt and C. A. Schmuttenmaer, "Far-infrared dielectric properties of polar liquids probed by femtosecond terahertz pulse spectroscopy," *Journal of Physical Chemistry*, vol. 100, no. 24, pp. 10373–10379, 1996.

[80] B. M. Fischer, M. Walther, and P. U. Jepsen, "Far-infrared vibrational modes of DNA components studied by terahertz time-domain spectroscopy," *Physics in Medicine and Biology*, vol. 47, no. 21, pp. 3807–3814, 2002.

[81] K. Ajito and Y. Ueno, "THz chemical imaging for biological applications," *IEEE Transactions on Terahertz Science and Technology*, vol. 1, no. 1, pp. 293–300, 2011.

[82] P. F. Taday, I. V. Bradley, D. D. Arnone, and M. Pepper, "Using Terahertz pulse spectroscopy to study the crystalline structure of a drug: a case study of the polymorphs of ranitidine hydrochloride," *Journal of Pharmaceutical Sciences*, vol. 92, no. 4, pp. 831–838, 2003.

[83] R. M. Woodward, B. E. Cole, V. P. Wallace et al., "Terahertz pulse imaging in reflection geometry of human skin cancer and skin tissue," *Physics in Medicine and Biology*, vol. 47, no. 21, pp. 3853–3863, 2002.

[84] A. G. Davies, A. D. Burnett, W. Fan, E. H. Linfield, and J. E. Cunningham, "Terahertz spectroscopy of explosives and drugs," *Materials Today*, vol. 11, no. 3, pp. 18–26, 2008.

[85] D. Zimdars, J. S. White, G. Stuk, A. Chernovsky, G. Fichter, and S. Williamson, "Large area terahertz imaging and non-destructive evaluation applications," *Insight*, vol. 48, no. 9, pp. 537–539, 2006.

[86] H. Hoshina, Y. Sasaki, A. Hayashi, C. Otani, and K. Kawase, "Noninvasive mail inspection system with terahertz radiation," *Applied Spectroscopy*, vol. 63, no. 1, pp. 81–86, 2009.

[87] M. C. Kemp, "Explosives detection by terahertz spectroscopy—a bridge too far," *IEEE Transactions on Terahertz Science and Technology*, vol. 1, no. 1, pp. 282–292, 2011.

[88] S. Wietzke, C. Jansen, F. Rutz, D. M. Mittleman, and M. Koch, "Determination of additive content in polymeric compounds with terahertz time-domain spectroscopy," *Polymer Testing*, vol. 26, no. 5, pp. 614–618, 2007.

[89] C. Jansen, S. Wietzke, O. Peters et al., "Terahertz imaging: applications and perspectives," *Applied Optics*, vol. 49, no. 19, pp. E48–E57, 2010.

[90] C. Jördens, S. Wietzke, M. Scheller, and M. Koch, "Investigation of the water absorption in polyamide and wood plastic composite by terahertz time-domain spectroscopy," *Polymer Testing*, vol. 29, no. 2, pp. 209–215, 2010.

[91] F. Rutz, M. Koch, S. Khare, M. Moneke, H. Richter, and U. Ewert, "Terahertz quality control of polymeric products," *International Journal of Infrared and Millimeter Waves*, vol. 27, no. 4, pp. 547–556, 2006.

[92] J. B. Jackson, J. Bowen, G. Walker et al., "A survey of terahertz applications in cultural heritage conservation science," *IEEE Transactions on Terahertz Science and Technology*, vol. 1, no. 1, pp. 220–231, 2011.

[93] D. Banerjee, W. von Spiegel, M. D. Thomson, S. Schabel, and H. G. Roskos, "Diagnosing water content in paper by terahertz radiation," *Optics Express*, vol. 16, no. 12, pp. 9060–9066, 2008.

[94] F. Hindle, A. Cuisset, R. Bocquet, and G. Mouret, "Continuous-wave terahertz by photomixing: applications to gas phase pollutant detection and quantification," *Comptes Rendus Physique*, vol. 9, no. 2, pp. 262–275, 2008.

[95] C. Jördens and M. Koch, "Detection of foreign bodies in chocolate with pulsed terahertz spectroscopy," *Optical Engineering*, vol. 47, no. 3, Article ID 037003, 2008.

[96] Y. Hua and H. Zhang, "Qualitative and quantitative detection of pesticides with terahertz time-domain spectroscopy," *IEEE Transactions on Microwave Theory and Techniques*, vol. 58, no. 7, pp. 2064–2070, 2010.

[97] R. Blundell and C. Y. E. Tong, "Submillimeter receivers for radio astronomy," *Proceedings of the IEEE*, vol. 80, no. 11, pp. 1702–1720, 1992.

[98] C. Kulesa, "Terahertz spectroscopy for astronomy: from comets to cosmology," *IEEE Transactions on Terahertz Science and Technology*, vol. 1, no. 1, pp. 232–240, 2011.

[99] M. van Exter, C. Fattinger, and D. Grischkowsky, "Terahertz time-domain spectroscopy of water vapor," *Optics Letters*, vol. 14, no. 20, pp. 1128–1130, 1989.

[100] Y. S. Lee, *Principles of Terahertz Science and Technology*, Springer, NewYork, NY, USA, 2009.

[101] D. H. Auston, "Picosecond optoelectronic switching and gating in silicon," *Applied Physics Letters*, vol. 26, no. 3, pp. 101–103, 1975.

[102] N. Katzenellenbogen and D. Grischkowsky, "Efficient generation of 380 fs pulses of THz radiation by ultrafast laser pulse excitation of a biased metal-semiconductor interface," *Applied Physics Letters*, vol. 58, no. 3, pp. 222–224, 1991.

[103] M. Ashida, "Ultra-broadband terahertz wave detection using photoconductive antenna," *Japanese Journal of Applied Physics*, vol. 47, no. 10, pp. 8221–8225, 2008.

[104] C. Baker, I. S. Gregory, W. R. Tribe et al., "Highly resistive annealed low-temperature-grown InGaAs with sub-500 fs carrier lifetimes," *Applied Physics Letters*, vol. 85, no. 21, pp. 4965–4967, 2004.

[105] J. Sigmund, C. Sydlo, H. L. Hartnagel et al., "Structure investigation of low-temperature-grown GaAsSb, a material for photoconductive terahertz antennas," *Applied Physics Letters*, vol. 87, no. 25, Article ID 252103, 3 pages, 2005.

[106] M. Suzuki and M. Tonouchi, "Fe-implanted InGaAs photoconductive terahertz detectors triggered by 1.56 μm femtosecond optical pulses," *Applied Physics Letters*, vol. 86, no. 16, Article ID 163504, 3 pages, 2005.

[107] B. Sartorius, H. Roehle, H. Künzel et al., "All-fiber terahertz time-domain spectrometer operating at 1.5 μm telecom wavelengths," *Optics Express*, vol. 16, no. 13, pp. 9565–9570, 2008.

[108] Palací and B. Vidal, "Distributed THz transmitter/receiver based on a 1. 5 μm Fiber Link," in *Proceedings of the 36th International Conference on Infrared, Millimeter and Terahertz Waves (IRMMW-THz)*, Houston, Tex, USA, October 2011.

[109] J. R. Demers, R. T. Logan Jr., and E. R. Brown, "An optically integrated coherent frequency-domain THz spectrometer with signal-to-noise ratio up to 80 dB," in *Proceedings of the International Topical Meeting on Microwave Photonics (MWP'07)*, pp. 92–95, Victoria, Canada, October 2007.

[110] M. Scheller, K. Baaske, and M. Koch, "Multifrequency continuous wave terahertz spectroscopy for absolute thickness determination," *Applied Physics Letters*, vol. 96, no. 15, Article ID 151112, 3 pages, 2010.

[111] H. J. Song, N. Shimizu, T. Furuta, K. Suizu, H. Ito, and T. Nagatsuma, "Broadband-frequency-tunable sub-terahertz wave generation using an optical comb, AWGs, optical switches, and a uni-traveling carrier photodiode for spectroscopic applications," *Journal of Lightwave Technology*, vol. 26, no. 15, pp. 2521–2530, 2008.

[112] A. Roggenbuck, H. Schmitz, A. Deninger et al., "Coherent broadband continuous-wave terahertz spectroscopy on solid-state samples," *New Journal of Physics*, vol. 12, Article ID 043017, 2010.

[113] D. Stanze, A. Deninger, A. Roggenbuck, S. Schindler, M. Schlak, and B. Sartorius, "Compact cw terahertz spectrometer pumped at 1.5 μm wavelength," *Journal of Infrared, Millimeter, and Terahertz Waves*, vol. 32, no. 2, pp. 225–232, 2011.

[114] T. Göbel, D. Schoenherr, C. Sydlo, M. Feiginov, P. Meissner, and H. L. Hartnagel, "Single-sampling-point coherent detection in continuous-wave photomixing terahertz systems," *Electronics Letters*, vol. 45, no. 1, pp. 65–66, 2009.

[115] S. Hisatake, G. Kitahara, N. Kukutsu, Y. Fukada, N. Yoshimoto, and T. Nagatsuma, "Phase-sensitive terahertz self-heterodyne systembased on photonic techniques," in *Proceedings of the IEEE International Topical Meeting on Microwave Photonics (MWP)*, 2012.

[116] http://www.rainbowphotonics.com/prod_teratune.php.

[117] http://www.teraview.com/products/terahertz-continuous-wave-cw400/index.html.

[118] http://www.toptica.com/products/terahertz_generation/lasers_and_photomixers_for_cw_terahertz_generation.html.

[119] http://emcorephotonicsystems.com/products/terahertz-thz-frequency-domain-spectrometer-ftir/.

[120] http://www.hhi.fraunhofer.de/en/departments/photonic-components/terahertz-generation-detection/.